Characterization of Rat Meibomian Gland Ion and Fluid Transport

Dongfang Yu,[1] Richard M. Davis,[2] Megumi Aita,[3] Kimberlie A. Burns,[1] Phillip W. Clapp,[1] Rodney C. Gilmore,[1] Michael Chua,[1] Wanda K. O'Neal,[1] Richard Schlegel,[4] Scott H. Randell,[1] and Richard C. Boucher[1]

[1]Marsico Lung Institute/UNC Cystic Fibrosis Research Center, School of Medicine, University of North Carolina at Chapel Hill, Chapel Hill, North Carolina, United States
[2]Department of Ophthalmology, The University of North Carolina, Chapel Hill, North Carolina, United States
[3]Neuroscience Center, The University of North Carolina, Chapel Hill, North Carolina, United States
[4]Department of Pathology, Georgetown University Medical School, Washington District of Columbia, United States

Purpose. We establish novel primary rat meibomian gland (MG) cell culture systems and explore the ion transport activities of the rat MG.

Methods. Freshly excised rat MG tissues were characterized as follows: (1) mRNA expression of selected epithelial ion channels/transporters were measured by RT-PCR, (2) localization of epithelial sodium channel (ENaC) mRNAs was performed by in situ hybridization, and (3) protein expression and localization of βENaC, the $Na^+/K^+/Cl^-$ cotransporter (NKCC), and the Na^+/K^+ ATPase were evaluated by immunofluorescence. Primary isolated rat MG cells were cocultured with 3T3 feeder cells and a Rho-associated kinase (ROCK) inhibitor (Y-27632) for expansion. Passaged rat MG cells were cultured as planar sheets under air-liquid interface (ALI) conditions for gene expression and electrophysiologic studies. Passaged rat MG cells also were cultured in matrigel matrices to form spheroids, which were examined ultrastructurally by transmission electron microscopy (TEM) and functionally using swelling assays.

Results. Expression of multiple ion channel/transporter genes was detected in rat MG tissues. β-ENaC mRNA and protein were localized more to MG peripheral acinar cells than central acinar cells or ductular epithelial cells. Electrophysiologic studies of rat MG cell planar cultures demonstrated functional sodium, chloride, and potassium channels, and cotransporters activities. Transmission electron microscopic analyses of rat MG spheroids revealed highly differentiated MG cells with abundant lysosomal lamellar bodies. Rat MG spheroids culture-based measurements demonstrated active volume regulation by ion channels.

Conclusions. This study demonstrates the presence and function of ion channels and volume transport by rat MG. Two novel primary MG cell culture models that may be useful for MG research were established.

Keywords: meibomian gland, cell culture, ion transport, electrophysiology

The meibomian gland (MG) is a modified sebaceous gland that resides within the upper and lower eyelids. The MG has an essential role in maintaining ocular surface health by providing the outer lipid layer of the tear film that protects the tear film from evaporation of the aqueous phase and stabilizes the tear film by lowering its surface tension.[1]

Meibomian gland dysfunction (MGD) is a chronic, but poorly understood, abnormality that is characterized commonly by terminal duct obstruction and/or qualitative/quantitative changes in the glandular secretion (meibum).[2] Meibomian gland dysfunction is a leading cause of dry eye, one of the most frequent diagnoses in ophthalmic clinics, which affects 4 to 6 million people in the United States.[3,4] Both MGD and dry eye generally have been accepted to be age-related diseases that predominantly affect female patients.[1,5–7] Age-related changes in MG function, including acinar dystrophy, ductal hyperkeratinization, and androgen deficiency, have been associated with

development of MGD.[8,9] Despite these findings, many questions remain about the pathogenesis and management of MGD.

Ion channels are expressed in the acinar and ductal compartments of most glands, and they are fundamental for secretion and modification of glandular liquids. Previous studies have characterized the presence of chloride, sodium, and potassium channels in acinar and ductal regions of the lacrimal gland.[10,11] Ion channels also coordinately provide conjunctival and corneal epithelia with the capacity to actively regulate tears produced by the lacrimal gland.[12–14] Recent studies have expanded the function of ion channels in epithelial homeostasis to include roles in sensing the extracellular microenvironment during maturation and regeneration.[15,16]

To our knowledge, the MG, as the major source of lipids for the tear film, has not been reported to exhibit active ion transport as part of its normal function. However, previous studies of subjects with a genetic loss of the epithelial sodium channel (ENaC) function, pseudohypoaldosteronism (PHA),

revealed visible white material protruding from MG orifices, strongly suggesting a role of ENaC in normal MG function.[17-19] Thus, we hypothesized that ENaC and other ion channels may have a critical role in the physiology and pathophysiology of the MG, based either on their Na^+, Cl^-, and volume transport, and/or microenvironmental sensing properties.

To provide a basis for understanding the role(s) of transepithelial ion transport in MG function, we first characterized the expression of sodium and chloride channels in freshly excised rat MG tissues. To generate adequate cell numbers for phenotypic characterization of ion transport, we developed a novel in vitro primary MG cell coculture model with rat MG cells and 3T3-swiss albino feeder cells in the presence of a Rho-associated kinase (ROCK) inhibitor (Y-27632).[20,21] A comprehensive series of pharmacologic studies was used to characterize the ion transport properties of MG cells cultured as planar sheets using Ussing chamber approaches and cultured as spheroids, optically measuring volume responses. This combination of approaches had two goals: to develop primary MG cell culture models useful for ion transport studies pertinent to MG research and to provide an understanding of the roles of ion channels in MG physiology.

MATERIALS AND METHODS

Animals

Male Sprague-Dawley rats (Charles River, Wilmington, MA, USA), weighing 250 to 300 g, were studied at age 10 to 12 weeks. Animals were studied in compliance with the Association for Research in Vision and Ophthalmology (ARVO) Statement for the Use of Animals in Ophthalmic and Vision Research, and protocols were approved by the Institutional Animal Care and Use Committee of the University of North Carolina at Chapel Hill.

Conventional and Real Time RT-PCR Analysis

To obtain tissue, rats were killed by CO_2 asphyxiation. Meibomian gland tissues were isolated under a dissecting microscope (Olympus Co., Tokyo, Japan) by removing the skin, connective tissue, muscle, palpebral conjunctiva, and eyelid margins. The resected MGs were homogenized with Minilys homogenizer (Bertin Technologies, Bordeaux, France) and extracted for total RNA with RNeasy Plus Mini Kit (Qiagen, Valencia, CA, USA) in accordance with the manufacturer's instructions. Messenger RNA expression of genes of interest, including rat epithelial sodium channel (*ENaC α*, *β*, and *γ* subunits), the sodium/glucose cotransporter 1 (*Slc5a1*), the cystic fibrosis transmembrane conductance regulator (*Cftr*), and members of the transmembrane protein 16 (*Tmem16a* and *f*, Ca^{2+} activated Cl^- channel), were studied by conventional and real time RT-PCR as described previously.[13] Other primers used were as follows: $Na^+/K^+/Cl^-$ cotransporter (NKCC; *Nkcc1*), 5′-tgttggattcgcagagactg-3′ (forward), 5′-cccagaagaaccaccactgt-3′ (reverse); Na^+/K^+ ATPase (*Atp1a1*), 5′-ctgggaggcttcttcacttatt-3′ (forward), 5′-atcttcctctgctcgtaggt-3′ (reverse); large-conductance Ca^{2+}-activated (Maxi-K^+) potassium channel (*BKCa*), 5′-cccaatagaatcctgccaga-3′ (forward), 5′-cagcttatcattggctgcaa-3′ (reverse); and L-type voltage-dependent calcium channel (*Cav1.2*), 5′-cgcaacggttggaatttact-3′ (forward), 5′-ctcagtgccttcacatcgaa-3′ (reverse).

In Situ Hybridization

Antisense and sense riboprobes were prepared from mouse ENaC cDNAs by RT-PCR with primer oligomers listed as follows:[19] αENaC, 5′-CTAATGATGCTGGACCACACC-3′ and 5′-AAAGCGTCTGTTCCGTGATGC-3′, with a product length of 556 base pairs (bp); βENaC, 5′-GCCAGTGAAGAAGTACCTCC-3′ and 5′-CCTGGGTGGCACTGGTGAA-3′, with a product length of 632 bp; and γENaC, 5′-AAGAATCTGCCCAGTTCGAGGC-3′ and 5′-TACCACTCCTGGATGGCATTG-3′, with a product length of 671 bp. These PCR products were cloned into the pCR-Blunt II-TOPO vector (Invitrogen Life Technologies, San Diego, CA, USA) and linearized with EcoRV and Hind III. Complimentary riboprobes were generated by in vitro transcription using digoxigenin RNA labeling mix (Roche Diagnostics, Indianapolis, IN, USA) and purified with Probe-Quant G-50 Micro Columns (GE Healthcare Bio-Sciences, Pittsburgh, PA, USA).

Frozen blocks of rat MG tissue embedded in the optimum-cutting temperature compound (OCT) were sectioned into 12-μm thick sections, which were mounted on silane-coated glass slides for in situ hybridization analysis according to a modified protocol.[22,23] The cryosections were fixed in 4% paraformaldehyde in diethy-pyrocarbonate (DEPC)-treated PBS for 15 minutes at room temperature, washed with PBS three times (5 minutes each time), then incubated with 0.25% acetic anhydride in 0.1 M riethanolamine (pH 8.0) at room temperature. After washing with DEPC-PBS, the slides were prehybridized in a hybridization buffer (50% formamide, 1 × digoxigenin blocking reagent [Roche Diagnostics], 100 μg/mL heparin, 1 mg/mL denatured baker's yeast tRNA, 5 × SSC, 0.1% CHAPS, 5 mM EDTA [pH 8.0], 0.1% Tween 20) at 60°C for 3 to 4 hours, and then hybridized with 1 μg/mL DIG riboprobes in hybridization buffer at 60°C for 14 to 16 hours. After hybridization, sections were washed once in 2 × SSC for 15 minutes at 60°C, three times in 0.2 × SSC for 20 minutes each at 60°C, and twice in PBS with 0.1% Triton X-100. Subsequently, the sections were placed in a blocking solution containing 10% sheep serum and 1 × digoxigenin blocking reagent in 1 × maleic acid buffer (Roche Diagnostics) for 1 hour at room temperature, followed by incubation with anti-digoxigenin Fab fragments conjugated with alkaline phosphatase (AP; 1:2000; Roche Diagnostics) in the blocking solution for 3 hours at room temperature. The slides then were washed three times with 1 × digoxigenin washing buffer (DIG wash and block buffer set; Roche Diagnostics) for 10 minutes each and incubated in 1 × digoxigenin detection buffer (Roche Diagnostics) for 10 minutes. The signals were developed in nitroblue-tetrazolium chloride/5-bromo-4-chloro-3-indolylphosphate (NBT/BCIP; Roche Diagnostics) solution in the dark overnight. After rinses with PBS, the slides were mounted in Faramount aqueous mounting medium (Dako, Carpinteria, CA, USA). The signal specificities of mRNA for each gene in the MG tissues were tested by using sense probes as negative controls.

Immunofluorescence

Frozen rat MG tissue sections were fixed with precooled 100% ethanol for 15 minutes at 4°C. After blocking in a solution composed of 5% donkey serum, 1% BSA, 1% gelatin, and 0.2% Triton X-100 for 2 hours at room temperature, sections were incubated with primary antibodies including anti-βENaC antibody (1:100; StressMarq Biosciences, Victoria, Canada), or rabbit IgG control (Vector Laboratories, Burlingame, CA, USA) diluted in 5% donkey serum, 1% BSA, and 1% gelatin at 4°C overnight. A secondary fluorescent antibody (Texas Red Affinity Pure Donkey Anti-Rabbit IgG, H+L; Jackson ImmunoResearch Laboratories, West Grove, PA, USA) was used for detection, with Hochest 33342 (Invitrogen Life Technologies) for nuclear counterstaining. Slides were mounted with Faramount aqueous mounting medium and imaged under confocal microscope (Leica TCS SP2; Leica Microsystem, Buffalo Grove, IL, USA).
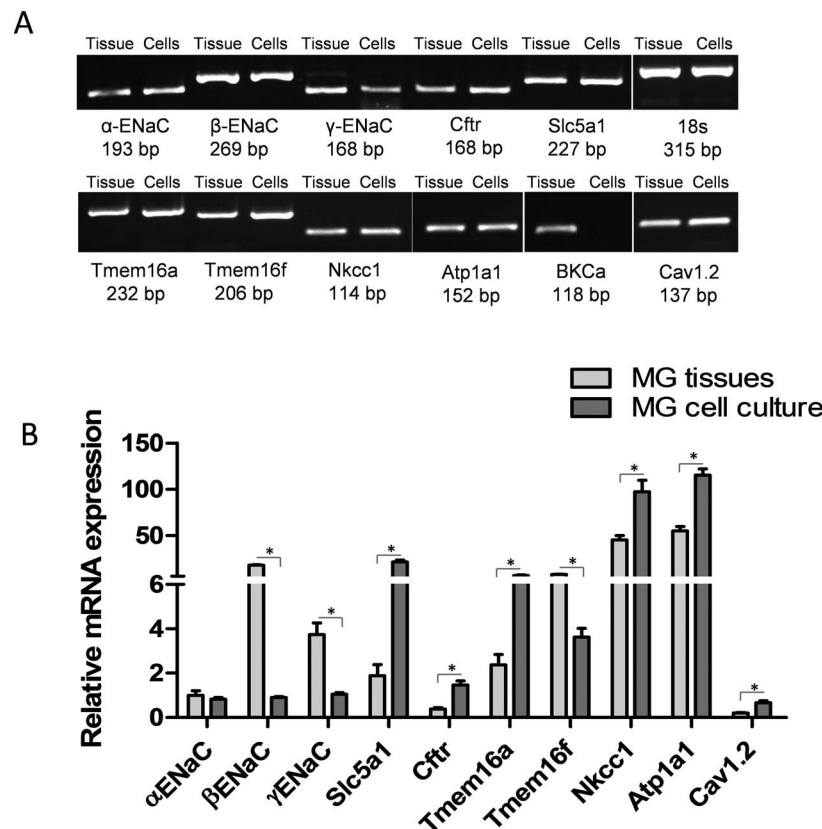
FIGURE 1. Ion channels/transporters gene expression in rat MG tissues and cell culture. (**A**) Conventional RT-PCR detected mRNA expression of selected genes, including α, β, and γ_ENaC_, _Slc5a1_, _Cftr_, _Tmem16a_ and _f_, _Nkcc1_, _Atp1a1_, _BKCa_, and _Cav1.2_, from freshly excised rat MG tissues. (**B**) Quantitative mRNA analysis by real-time PCR. Among the three subunits of ENaC, _βENaC_ mRNA was expressed more abundantly than α_ENaC_ and γ_ENaC_ in MG tissues. Comparison of rat MG tissues with cell cultures revealed a higher level of _βENaC_, γ_ENaC_, and _Tmem16f_, and lower levels of _Slc5a1_, _Cftr_, _Tmem16a_, _Nkcc1_, _Atp1a1_, and _Cav1.2_ mRNA in rat MG tissues than in cell cultures. No statistical differences were found regarding the expression levels of αENaC in rat MG tissues and cell cultures. *$P < 0.05$.

Frozen rat tissues, rat MG cell planar cultures on Snapwells, and MG spheroids cultures were fixed with 4% paraformaldehyde for 20 minutes at room temperature. After blocking, fixed tissues/cells were incubated with anti-NKCC1 (1:200; Abcam, Cambridge, MA, USA), and anti- Na$^+$/K$^+$ ATPase (1:200; Abcam) at 4°C overnight. Alexa Fluor 488 AffiniPure Goat Anti-Rabbit IgG (H+L; Jackson ImmunoResearch Laboratories) was used for detection, with the rest of steps same as described above.

Rat MG Cell Coculture With 3T3 Feeder Cells and a Rho Kinase Inhibitor

The 3T3 Swiss albino (SA) fibroblasts (American Type Culture Collection [ATCC], Manassas, VA, USA) were maintained in Dulbecco's modified Eagle medium (DMEM; Cellgro, Manassas, VA, USA) supplemented with 10% fetal bovine serum (Gibco Life Technologies, San Diego, CA, USA), 100 U/mL penicillin, and 100 μg/mL streptomycin. The fibroblast cells were growth arrested by treatment with 4 μg/mL mitomycin C (Sigma-Aldrich Corp., St. Louis, MO, USA) for 2 hours in a 37°C incubator and harvested with trypsin digestion. 3T3 SA cells were plated onto plastic culture dishes precoated with human placental type IV collagen (Sigma-Aldrich Corp.) for later coculture with rat MG cells.

Rat MG tissues were resected as described above. Tissues were digested with 2 mg/mL collagenase (Sigma-Aldrich Corp.) and 0.2 mg/mL dispase II (Roche Diagnostics) at 37°C for 2 hours.[21,24,25] Cell suspensions were dissociated into single cells by Accutase (Innovative Cell Technologies, Inc., San Diego, CA, USA) treatment for 25 minutes. Isolated MG cells were cocultivated with mitomycin C-treated 3T3 fibroblasts in F medium (DMEM/Nutrient Mixture F-12 3:1 [vol/vol], supplemented with 5% fetal bovine serum, 0.4 μg/mL hydrocortisone [Sigma-Aldrich Corp.], 5 μg/mL insulin [Sigma-Aldrich Corp.], 8.4 ng/mL cholera toxin [Sigma-Aldrich Corp.], 10 ng/mL epidermal growth factor [Invitrogen], 0.25 μg/mL amphotericin B [Sigma-Aldrich Corp.], 10 μg/mL gentamicin [Sigma-Aldrich Corp.], and 10 μmol/L Y-27632 [Enzo Life Sciences, Farmingdale, NY, USA]).[20] Y-27632 is ROCK inhibitor that promotes epithelial cell proliferation.[20] All cells were maintained at 37°C in a humidified incubator with 95% O_2 and 5% CO_2.

Differential Accutase digestion was used to separate 3T3 feeder cells and rat MG epithelial cells during passaging. Briefly, feeder:MG cocultures were rinsed with PBS and incubated with Accutase at 37°C in an incubator for 5 to 6 minutes, with close monitoring by phase contrast microscopy. Detached feeder cells were removed by aspiration, with MG epithelial cells remaining adherent to the culture dish. The MG epithelial cells were rinsed with PBS and then redigested with Accutase at 37°C for 20 to 25 minutes. Cells were harvested and resuspended in medium for subculture or in cryopreservation medium for freezing.

Air-Liquid Interface (ALI) Culture of Rat MG Cells

For ALI culture, passage 2 rat MG epithelial cells were seeded onto collagen precoated 12 mm permeable Snapwell inserts

α-ENaC	β-ENaC	γ-ENaC
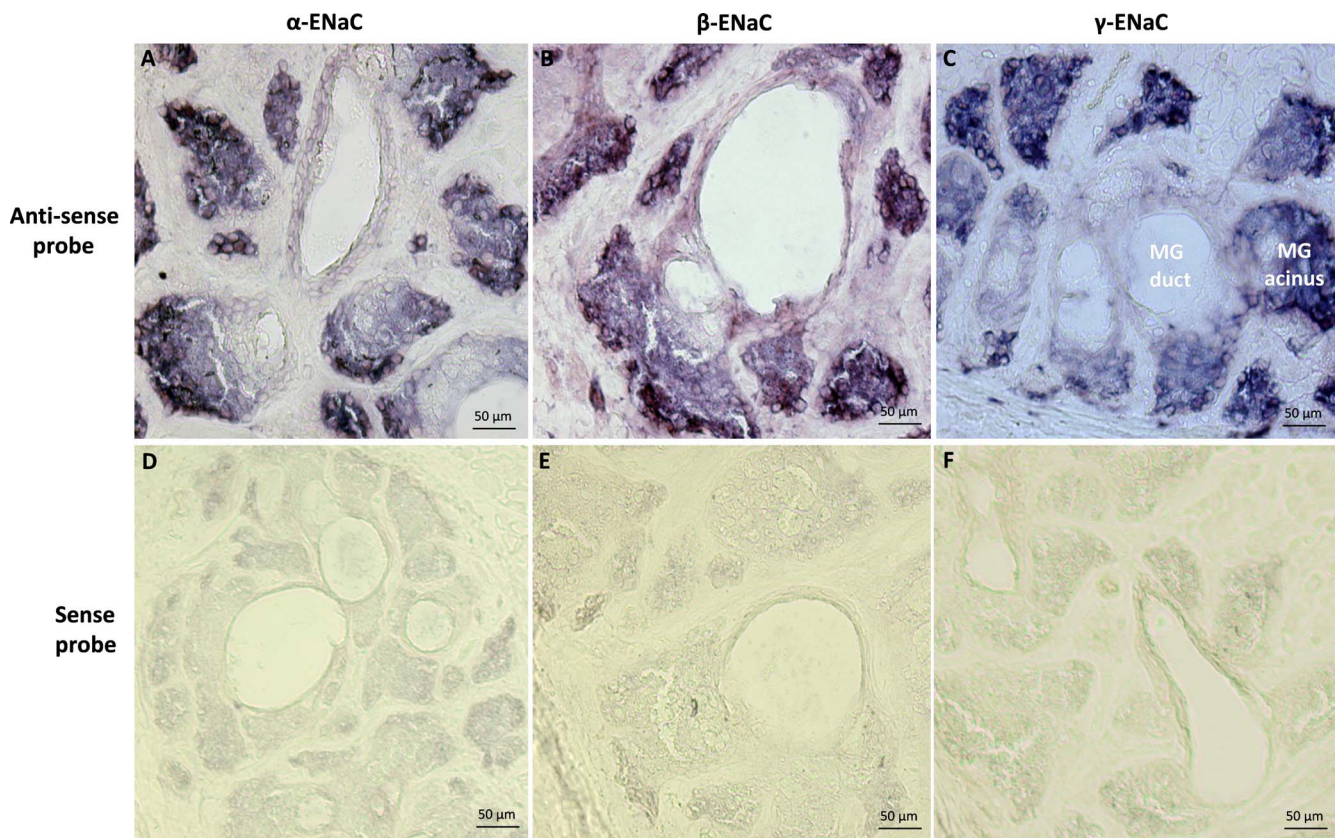
FIGURE 2. Localization of ENaC subunit (α, β, and γ) mRNA in rat MG tissues by in situ hybridization. In tissue, hybridization signals (*purple blue color*) for all three subunits of ENaC mRNA were detected in MG acinar cells, while the signals in the duct/ductule were much weaker (**A–C**). ENaC mRNA abundance decreased from peripheral acinar cells to acinar cells close to ductules/ducts. The sense probes did not yield specific staining (**D– F**).

(Corning-Costar, Cambridge, MA, USA) at a density of 120 k/ well in F medium.[20] On the following day, cells were fed with differentiation medium (DMEM/F-12 1:1 [vol/vol; Invitrogen Life Technologies], supplemented with 2% Ultroser G [Pall Corporation, Port Washington, NY, USA], 2% HyClone Fetal-Clone II Serum [GE Healthcare Bio-sciences, Pittsburgh, PA, USA], 22.5 μg/mL bovine brain extract [Lonza, Hopkinton, MA, USA], 2.5 μg/mL transferrin [Invitrogen Life Technologies], 2.5 μg/mL insulin [Sigma-Aldrich Corp.], 20 nM hydrocortisone [Sigma-Aldrich Corp.], 500 nM 3,3′,5-Triiodo-L-thyronine sodium salt [Sigma-Aldrich Corp.], 1.5 μM epinephrine [Sigma-Aldrich Corp.], 10 nM retinoic acid [Sigma-Aldrich Corp.], 250 nM O-Phosphorylethanolamine [Sigma-Aldrich Corp.], 250 nM ethanolamine [Sigma-Aldrich Corp.], 100 U/mL penicillin [Sigma-Aldrich Corp.], and 100 μg/mL streptomycin [Sigma-Aldrich Corp.]). Three days after seeding, the apical medium was removed to create ALI cultures, which were maintained for one additional week.

Generation and Structural Characterization of Three-Dimensional (3D) Spheroid Cultures of Rat MG Cells

Rat MG passage 2 cells were mixed well with Matrigel matrix (BD Biosciences, San Jose, CA, USA) and seeded onto Matrigel-precoated Nunc Lab-Tek 4-well chamber slides (Fisher scientific). After the cell-Matrigel mixture gelled in a 37°C incubator, 0.5 mL pre-warmed F medium was added to each chamber. Medium was replaced three times every week. Nine days later, the medium was switched to differentiation medium and cell

cultures were maintained for an additional 9 to 12 days for further analysis.

For histologic studies, MG cell spheroids were collected with BD cell recovery solution (BD Biosciences) according to the manufacturer's instructions. Meibomian gland cell pellets were embedded in OCT for frozen sections and immunofluorescence. Meibomian gland cell pellets also were fixed in 10% neutral buffered formalin overnight at room temperature, embedded in 2% agarose, and processed for hematoxylin and eosin (H&E) staining.

For electron microscopy, MG 3D culture pellets were fixed in 2% glutaraldehyde plus 2% paraformaldehyde in 0.1 mol/L Sorenson's phosphate buffer (pH 7.4) overnight at 4°C. Subsequently, the cell pellets were embedded in 2% agarose and postfixed in 1% osmium tetroxide (OsO_4) in 0.1 mol/L Sorenson's phosphate buffer (pH 7.4) for 1 hour. The cell pellet blocks then were dehydrated through a graded series of ethanols and propylene oxide, embedded in Poly/Bed 812 BDMA Mini Kit (Polysciences, Warrington, PA, USA), and sectioned on a Reichert ultramicrotome (Reichert Ultracut S; Leica Microsystem, Inc., Buffalo Grove, IL, USA) to obtain semithin sections. Next, the sections were stained with 2% methylene blue in 2% sodium borate and examined under a light microscope to select Epon blocks. The blocks then were used to prepare 90 nm thick ultrathin sections, which were placed on grids, double stained with uranyl acetate and lead citrate, examined, and photographed via an Opton EM 900 transmission electron microscope (TEM; Zeiss, Oberkochen, Germany).[26,27]
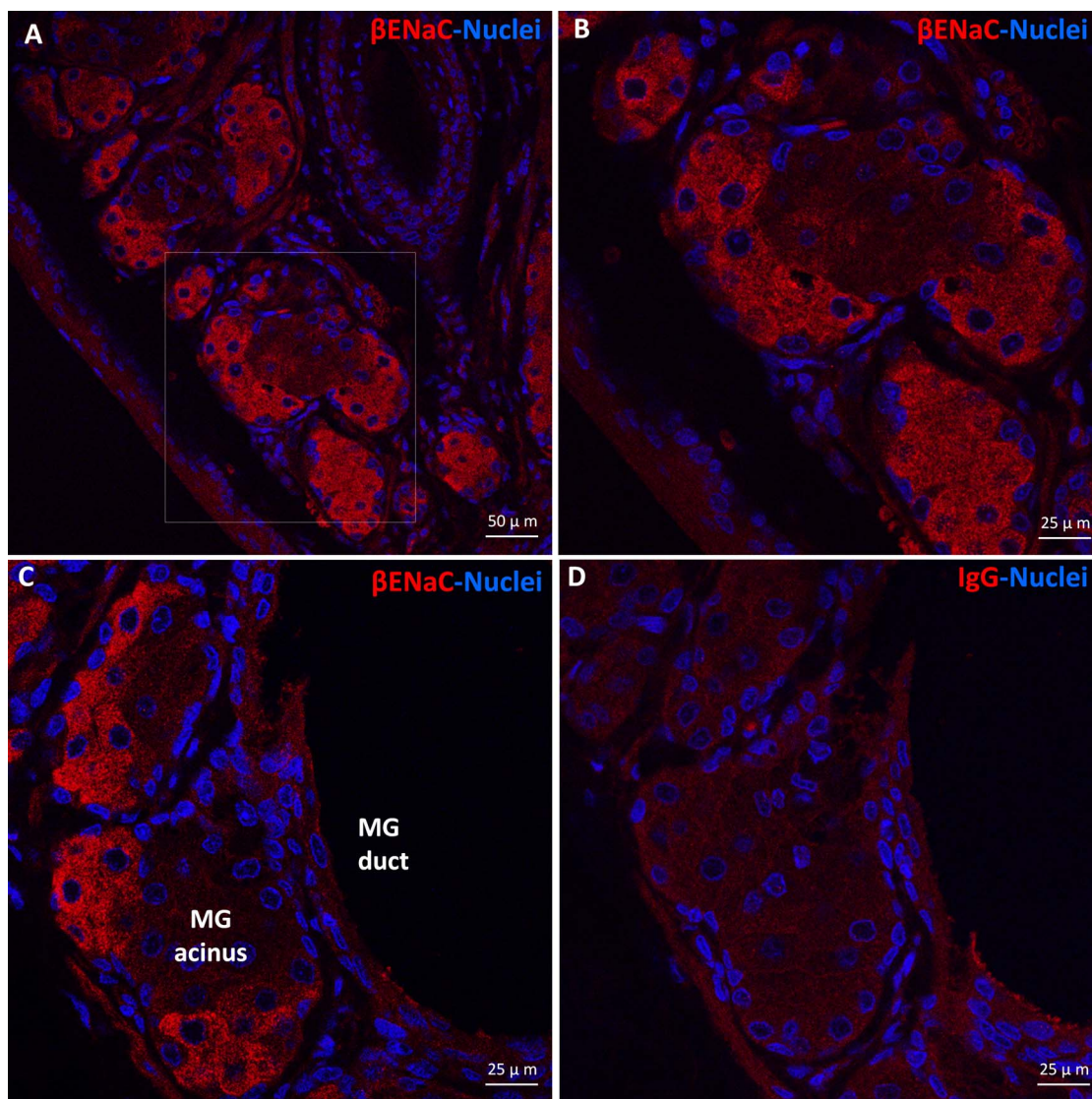
FIGURE 3. Immunolocalization of βENaC protein in rat MG tissues. βENaC protein (*red color*) was detected in rat MG acinar cells but was barely visible in ductal epithelial cells (**A–C**). (**B**) Higher magnification (×40) picture of the framed area in (**A**) (×20). Negative control (**D**).

Nile Red Staining

Stock solutions of Nile Red were prepared at 10 mg/mL in dimethyl sulfoxide (DMSO) and stored protected from light. Frozen rat tissue and MG sphere culture sections, and rat MG cell ALI cultures on Snapwells were fixed with 4% paraformaldehyde for 20 minutes at room temperature. After wash, fixed tissues/cells were incubated within 10 μg/mL Nile Red in PBS for 2 to 3 hours at room temperature and in the dark. The slides then were washed with PBS, mounted with Fluoroshield with DAPI histology mounting medium (Sigma-Aldrich Corp.), and imaged under confocal microscope.

Ussing Chamber Measurement of Rat MG Planar Cultures

Seven days after ALI culture was initiated, rat MG epithelial cell Snapwell cultures were mounted in Ussing chambers (Physiologic Instruments, San Diego, CA, USA) for bioelectric measurements. As previously described,[19] cells were bathed bilaterally with Krebs-bicarbonate Ringer (KBR) buffer at 37°C, bubbled with 95% O_2 to 5% CO_2 aeration to maintain the pH at 7.4. Short-circuit current (Isc) was recorded as the current required to null the transepithelial voltage to zero. The cultures were pulsed to $\pm$ 5 mV for 0.2-second duration every 20 seconds to calculate transepithelial resistance (R_T). The R_T and Isc were recorded continuously on a computer and analyzed with Acquire and Analysis software (Physiologic Instruments).

To identify functions of selected ion channels, agonists and antagonists were used, including: amiloride (ENaC inhibitor, 100 μM), phloridzin (sodium/glucose cotransporter inhibitor, 200 μM), forskolin (cystic fibrosis transmembrane conductance regulator [CFTR] activator, 10 μM), CFTRinh172 (CFTR inhibitor, 10 μM), UTP (TMEM16 activator, 10 μM), paxilline (high-conductance Ca^{2+}-activated [Maxi-K^+] potassium channel inhibitor, 10 μM), bumetanide ($Na^+/K^+/Cl^-$ co-transporter inhibitor, 100 μM), and N-(4-trifluoromethylphenyl) anthranilic acid (TFMP; TMEM16 inhibitor, 50 μM).[19] Compounds were applied sequentially to the mucosal bath except bumetanide, which was applied
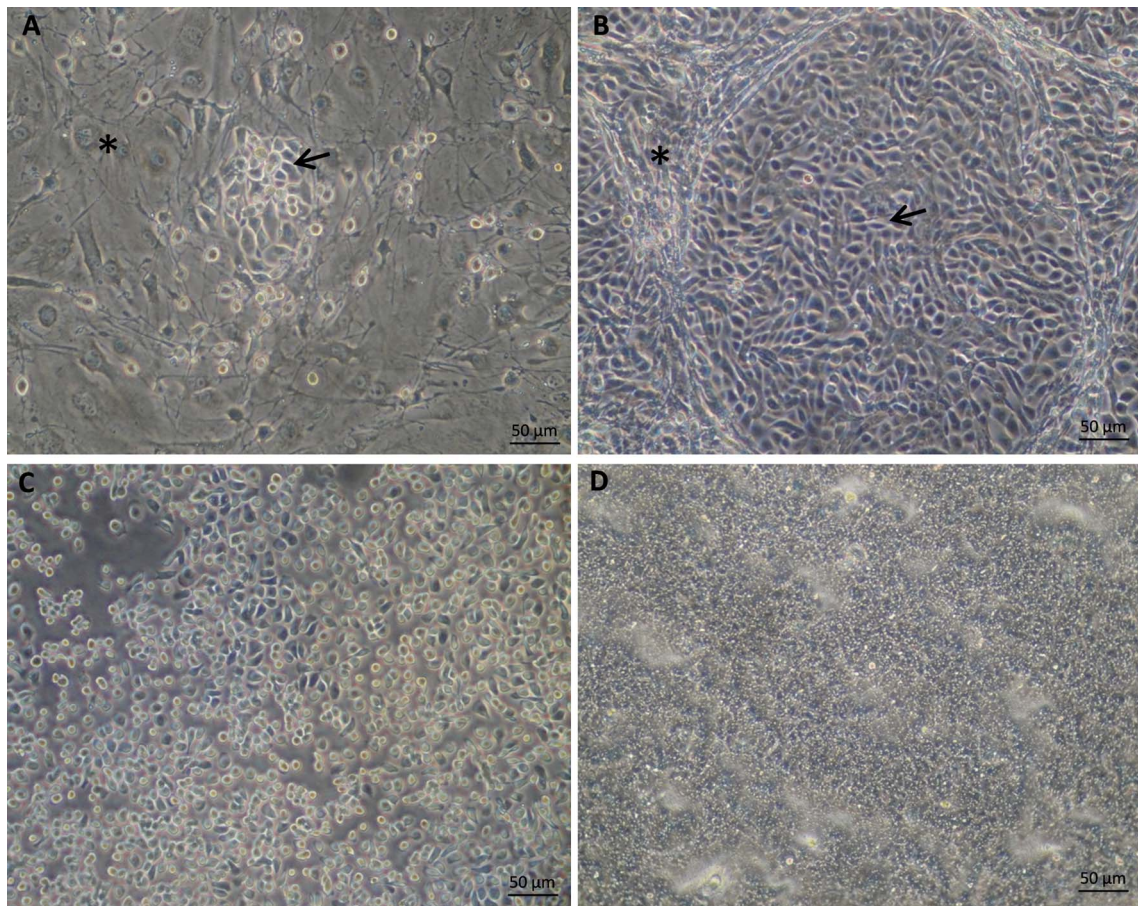
FIGURE 4. Appearance of primary rat Mebiomian gland cells culture. (**A**). Rat MG epithelial cells cocultured with 3T3-Swiss albino fibroblast feeder cells in F medium with ROCK inhibitor (Y-27632). (**B**) Confluent rat MG epithelial cells cocultured with feeder cells and Y-27632. (**C**) Rat MG cells under Accutase digestion with feeder cells detached earlier. (**D**) Rat MG cells under ALI culture in differentiation medium without feeder cells and Y-27632. The *asterisk* and *arrow* indicate feeder cells and rat MG cells, respectively.

to the serosal side. All compounds were obtained from Sigma-Aldrich Corp.

Functional Analysis of 3D Spheroid Culture of Rat MG Cells

Rat MG spheroids were treated with 2 μg/mL calcein green (Life Technologies) and 10 μg/mL Nile Red (Sigma-Aldrich Corp.) for 1 hour and imaged by confocal live-cell microscopy (FV1000, Olympus Co.). Spheroids then were treated with 10 μM forskolin, 5 μM benzamil (an ENaC inhibitor), 20 μM ouabain (Na^+/K^+ ATPase inhibitor), and 100 μM acetylcholine, overnight and reimaged on the following day. The maximal cross-sectional area of projection of spheroids was analyzed by Image J software (http://imagej.nih.gov/ij/; provided in the public domain by the National Institutes of Health, Bethesda, MD, USA) and compared before and after drug treatment.

Statistical Analysis

Data were described as mean ± SEM. Unpaired *t*-tests were used to compare the mRNA expression levels of genes of interest between freshly isolated rat MG tissues and cell culture. Unpaired *t*-tests also were used to compare the sizes of spheroid culture before and after drug treatment. Short-circuit current (Isc) changes caused by drug treatments were analyzed by paired *t*-test (before and after treatment). $P < 0.05$ was considered significant.

RESULTS

Gene Expression of Ion Channels/Transporters in Rat MG Tissues

The expression of the major epithelial ion channels and transporters, including α, β, and γ ENaC subunits, *Slc5a1*, *Cftr*, *Tmem16a* and *f*, *Nkcc1*, *Atp1a1*, *BKCa*, and *Cav1.2*, was evaluated in freshly isolated rat MG tissues by RT-PCR. As shown in Figure 1, all genes of interest were expressed in rat MG tissues. Relative mRNA levels of each gene quantitated by qPCR were obtained by normalizing to the *18s rRNA* gene (Fig. 1B). As typically observed in epithelia, the cotransporters and pumps were more highly expressed than channels. Perhaps uniquely, the β subunit of ENaC was more highly expressed than the α or γ subunit in MG tissues.[28]

Distribution of ENaC mRNA and Protein in Rat MG Tissues

We performed in situ hybridization to localize the mRNA distributions of the α, β, and γ subunits of ENaC in the MG. As shown in Figure 2, there was intense staining (purple blue color) of all three subunits of ENaC mRNA in MG acinar cells, while the staining in the duct/ductule was much weaker. Importantly, ENaC mRNA expression was greatest in peripheral acinar cells, was reduced in acinar cells apposed to the lumen,
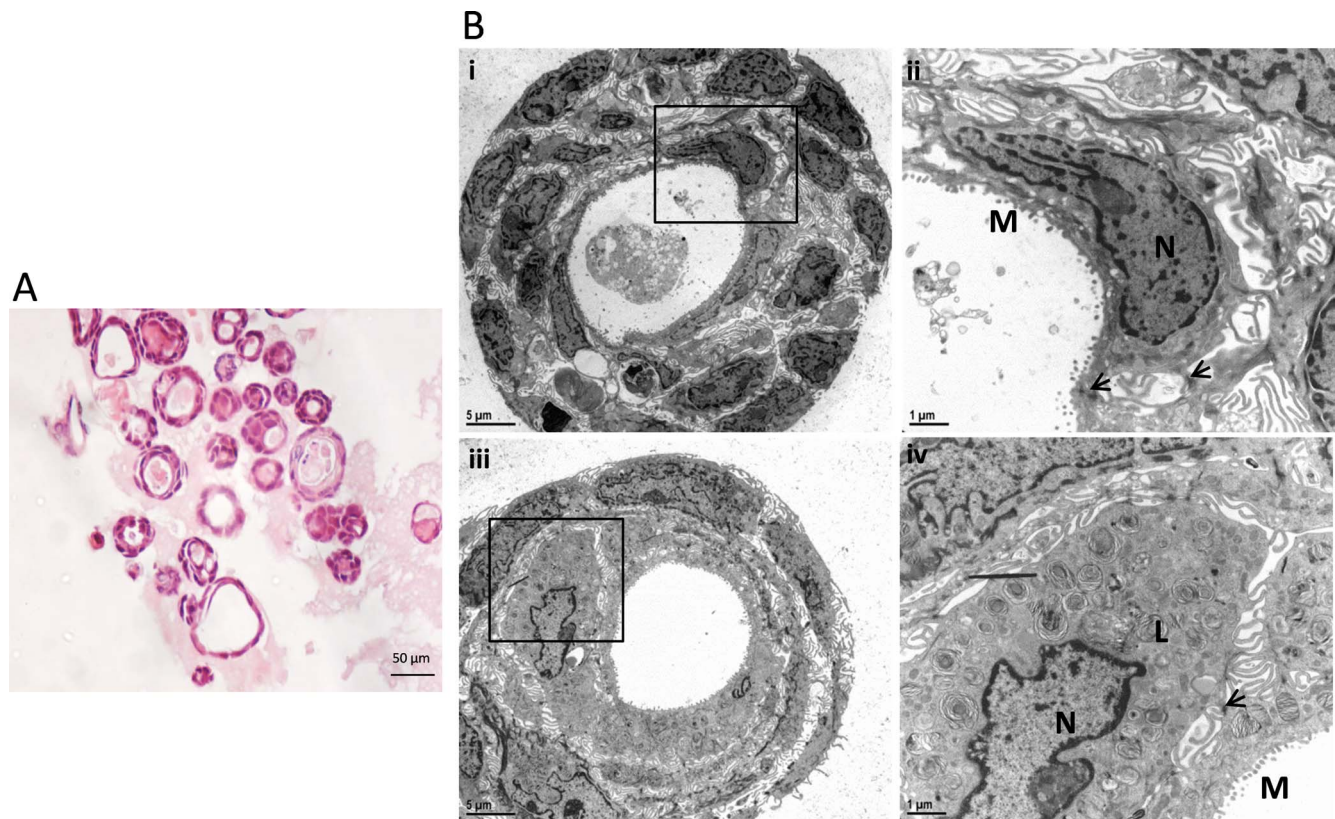
FIGURE 5. Histology and ultrastructure of rat MG cell 3D cultures examined by light microscopy and TEM. (**A**) Light microscopy of H&E-stained MG cell spheroids. The spheroids comprised 1 to 3 cell layers. (**B**) Transmission electron microscopy study of MG cell spheroids. *Bii* and *Biv* are higher power (×1000) views of the framed area in *Bi* and *Biii* (×200), respectively. *Bi* and *Bii* show MG cell spheroids with rich microvilli (*M*), tight junction (*arrows*), and secretory products with cell debris inside the lumen. *Biii* and *Biv* show a MG cell with pyknotic nuclei and an abundance of lysosomal lamellar bodies (*L*), which are markers of highly differentiated meibocytes. N, Nuclei.

and appeared lowest in ductules/ducts. The sense probe did not produce specific staining (Fig. 2).

Our immunofluorescence results revealed a distribution pattern of βENaC protein in rat MG tissues similar to the in situ hybridization of βENaC mRNA. As shown in Figure 3, βENaC protein was mostly highly expressed by acinar cells, particularly peripheral acinar cells. The IgG antibody-negative control did not reveal specific staining. Staining of α- and γ-ENaC protein was not successful, possibly due to the lower expression levels and/or lower affinity of the antibodies that we used.

Primary Rat MG Cell Coculture With Feeder Cells and a Rho Kinase Inhibitor

Rat MG cells were cocultured with growth-arrested 3T3 feeder cells in combination with a Rho kinase inhibitor (Y-27632) on plastic culture dishes for expansion. As shown in Figure 4A, rat MG cells cultured on tissue culture plastic formed colonies composed of small, bright, ovoid or polygonal epithelial cells among feeder cells. Cells proliferated rapidly under this system. Confluent epithelial colonies exhibited a cobblestone morphology (Fig. 4B). Cells were subcultured by differential Accutase digestion based on the observation that 3T3 feeder cells detached rapidly under Accutase digestion. Figure 4C shows a representative photograph of MG cells during enzyme digestion after feeder cells had been removed. Rat MG epithelial cells proliferated rapidly and survived through at least 6 passages under these conditions.

Characterization of Rat MG Cells in Planar Culture

Passage 2 rat MG cells were plated onto permeable Snapwell inserts and were subjected to ALI culture to induce differentiation (Fig. 4D) after reaching confluence. Seven days after ALI culture, cells growing on Snapwells were used for studies. Meibomian gland cells cultured under ALI conditions were initially characterized for gene expression levels of selected ion channels, as compared to freshly isolated MG tissues. As shown in Figure 1B, the levels of $\alpha ENaC$ mRNAs were comparable between MG cell cultures and tissues, whereas the levels of $\beta ENaC$, $\gamma ENaC$, and $Tmem16f$ mRNA were lower in MG cell cultures than in freshly isolated tissues ($P < 0.05$). In contrast, the levels of $Slc5a1$, $Cftr$, $Tmem16a$, $Nkcc1$, $Atp1a1$, and $Cav1.2$ mRNA were significantly higher in MG cell cultures compared to in vivo tissues ($P < 0.05$). We detected $BKCa$ mRNA expression in rat MG tissues, but not the cultured MG cells.

Histologic Characterization of Three-Dimensional Rat MG Spheroid Cultures

Passaged MG cells were seeded in matrigel matrices without feeder cells (9 days in F medium with Y-27632 and 12 days in differentiation medium without Y-27632). Histologic analysis revealed that MG cells had formed spheroids at 3 weeks, which were composed of 1 to 3 cell layers (Fig. 5A). Ultrastructural examination by TEM revealed that MG spheroids were rich in microvilli, tight junctions, and secretory products, with cell debris within the lumen (Fig. 5B). There were highly differentiated MG cells with pyknotic nuclei and an abundance
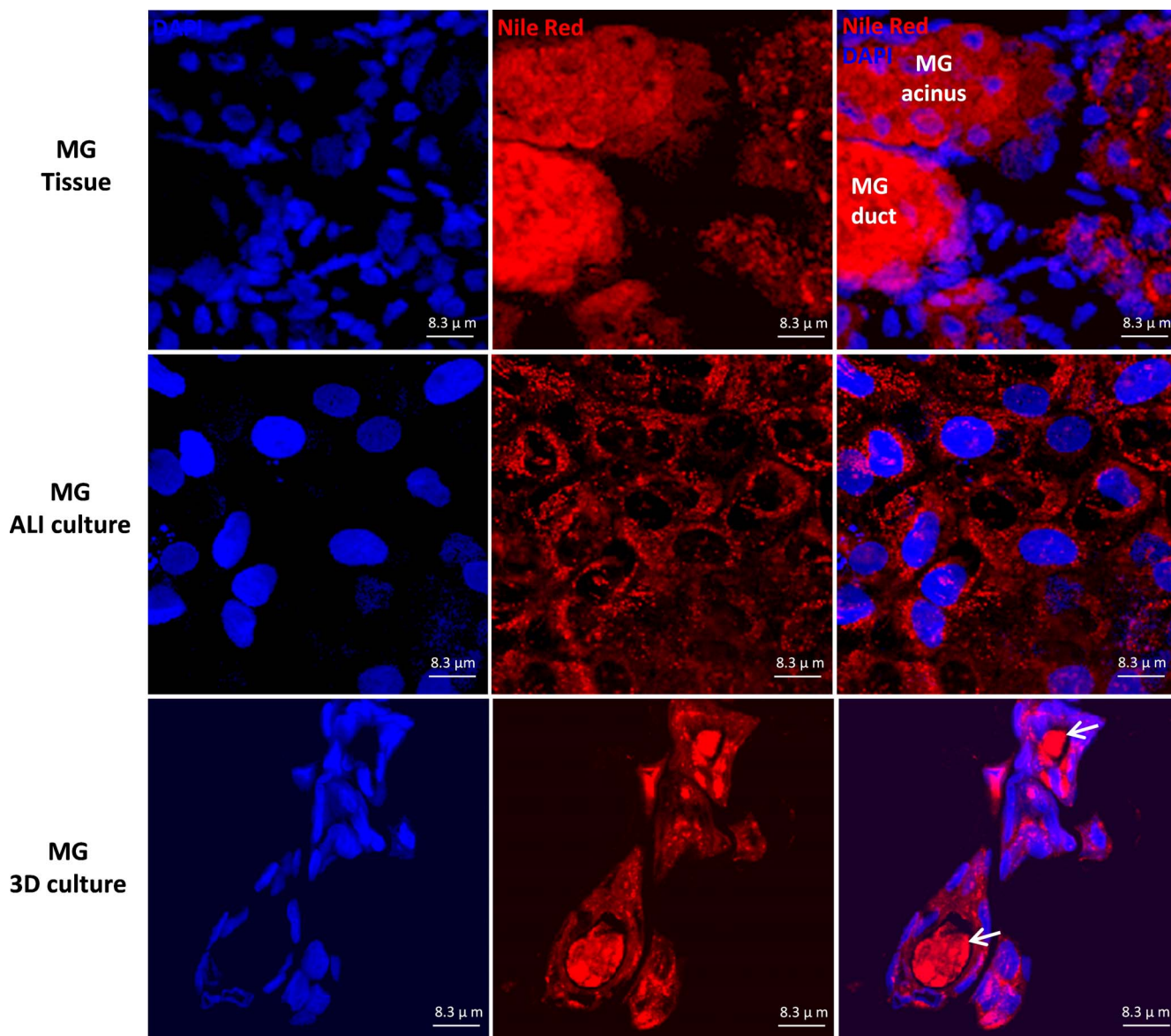
FIGURE 6. Nile Red staining of rat MG tissues, MG ALI cultures, and MG spheroid cultures. Positive Nile Red staining was revealed in the cytoplasm of acinar cells of rat MG tissues and cultured MG cells. In rat MG 3D culture, there were secretions in the lumen of the spheres stained positive, which indicated lipid components of the secretions (*arrows*).

of lysosomal lamellar bodies, which are markers of mature meibocytes (Fig. 5B).

Nile Red Staining and Immunostaining of NKCC and Na⁺/K⁺ ATPase in Planar and Spheroid Cultures

We compared lipid staining and ion channel immunostaining in rat MG tissues and primary cell planar and spheroid cultures. As shown in Figure 6, Nile Red staining revealed strong intracellular lipid staining in acinar cells of rat MG tissues and both types of cultured MG cells. In rat MG tissues, secretions inside the lumina of MG duct exhibited extremely strong Nile Red staining signal. Similarly, the secretions inside the lumina of the rat spheroid culture also were stained positively by Nile Red, consistent with a lipid component of the intraluminal secretions.

Immunoreactivity of NKCC was observed in all MG epithelial cell types, but was observed more strongly in the ductal epithelial cells than acinar cells of rat MG tissues (Fig. 7). In rat MG cell cultures, positive NKCC immunoreactivity was revealed in most cultured rat MG cells under planar and spheroid conditions. Immunostaining of Na^+/K^+ ATPase revealed strong signals in the plasma membrane of ductal epithelial and acinar cells of rat MG tissues, which were comparable (Fig. 8). Similar immunolocalization of Na^+/K^+ ATPase was observed in the plasma membrane of rat MG cells under planar and spheroid culture.

Based on the detection of Nile Red/lysosomal lamellar bodies, Na^+/K^+ ATPase, and NKCC positive cells in planar and spheroid cultures, it is likely that the planar and spheroid cultures were dominated by acinar cells but we cannot rule out a component of ductal cells.

Bioelectric Properties of Primary Rat Meibomian Planar Gland Cell Cultures

Meibomian gland cell cultures on Snapwells were mounted in Ussing chambers to study the ion transport properties of MG
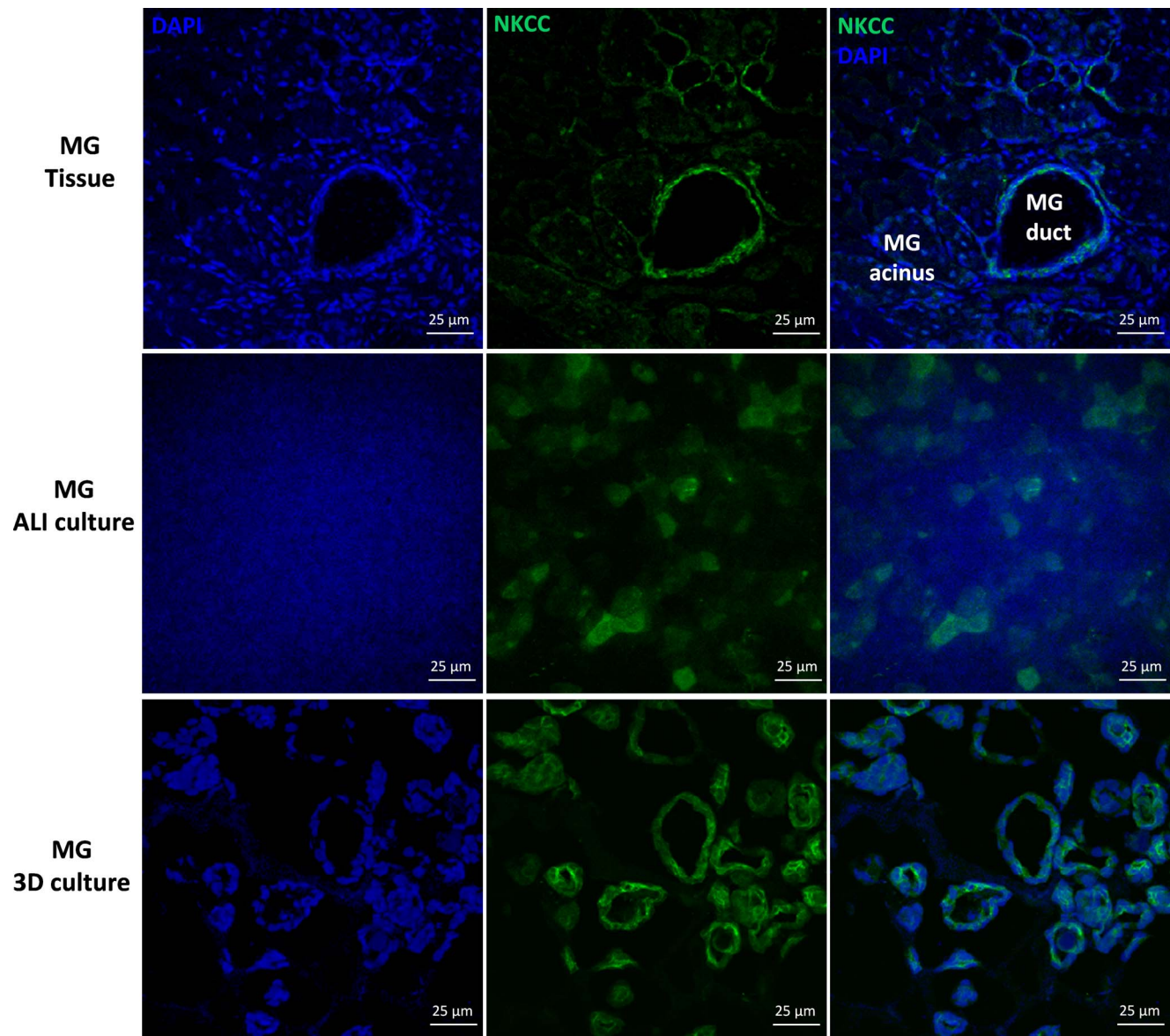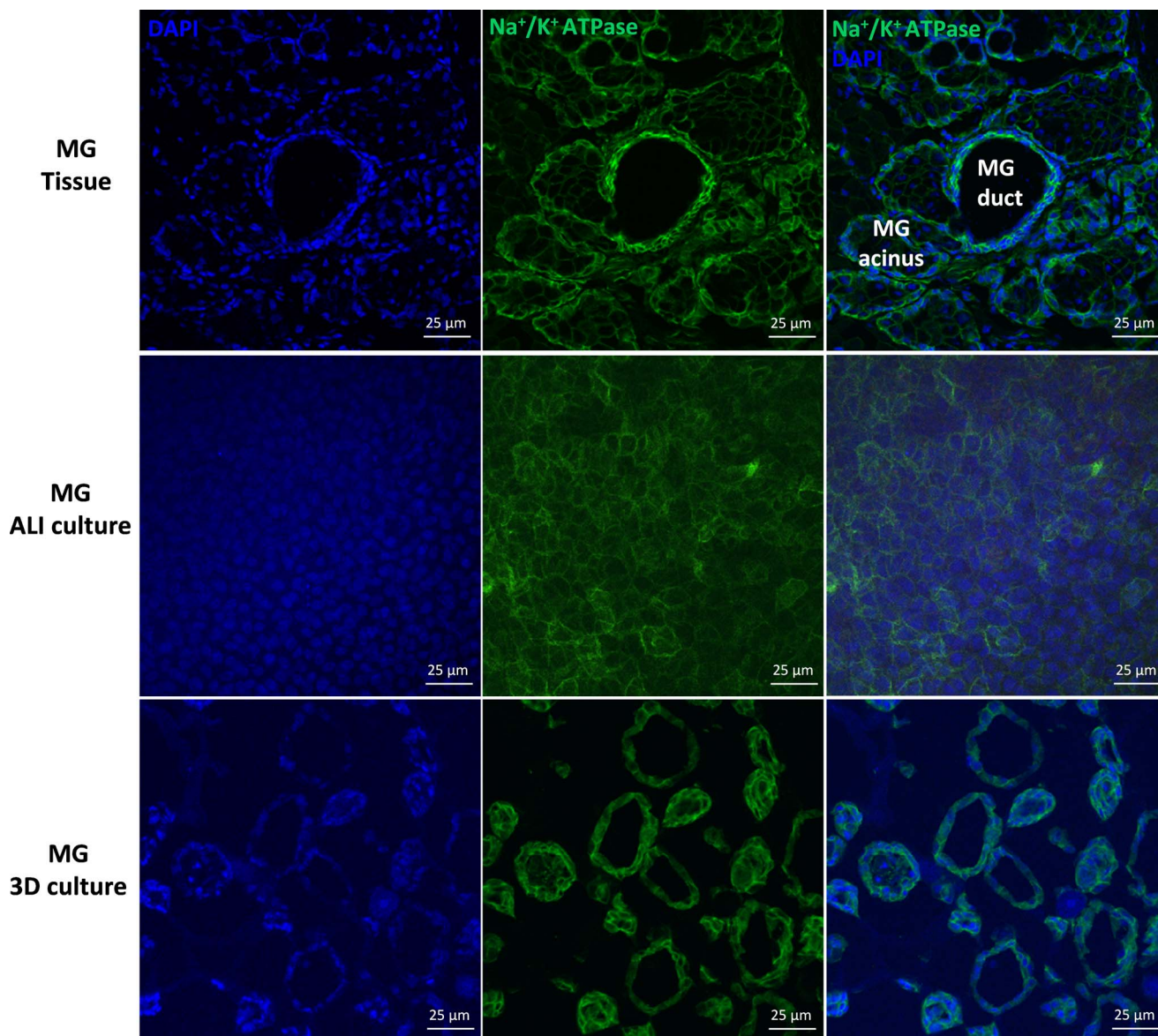
FIGURE 7. Immunolocalization of the NKCC in rat MG tissues, MG ALI cultures, and MG spheroid cultures. Na$^+$/K$^+$/Cl$^-$ cotransporter was expressed in rat MG ductal epithelial and acinar cells. In rat MG cell culture, positive immunoreactivity was revealed in most cultured rat MG cells.

epithelia. Six Snapwells of cells from three different tissue isolations were analyzed for basal bioelectric parameters, including PD, R_T, and Isc, and responses to a series of agonists/inhibitors as discussed in Methods. Meibomian gland cells exhibited a basal transepithelial PD of -5.8 ± 0.78 mV, an Isc of 3.2 ± 0.47 μA/cm^2, and R_T of 814 ± 151 $\Omega \cdot$cm^2.

The ENaC inhibitor, amiloride, and phloridzin (a sodium/glucose cotransporter inhibitor) inhibited Isc by -0.7 ± 0.23 and -1.4 ± 0.08 μA/cm^2, respectively ($P < 0.05$; Fig. 9). With respect to Cl$^-$ secretion, the Isc response to forskolin was the largest among the tested compounds, with a statistically significant ΔIsc of 7.2 ± 0.47 μA/cm^2 ($P < 0.05$). The increased Isc waned modestly within several minutes and then remained stable at a level above forskolin pretreatment. CFTRinh172 decreased the Isc significantly by -3.6 ± 0.17 μA/cm^2 ($P < 0.05$). The Ca^{2+}-activated chloride channel (TMEM16A) activator, UTP, elicited a transient increase in Isc of 0.6 ± 0.16 μA/cm^2 ($P < 0.05$), which waned within a few

minutes. Paxilline, a BKCa inhibitor, caused a slight but significant decrease of Isc by -0.5 ± 0.13 μA/cm^2 ($P < 0.05$). Considering the undetectable level of BKCa mRNA in cultured rat MG cells (Fig. 1), this inhibition of Isc caused by paxilline might be due to a nonspecific effect on other ion transport–related molecules. The application of bumetanide (Na$^+$/K$^+$/Cl$^-$ cotransporter inhibitor) caused a slight and insignificant decrease of Isc by -0.2 ± 0.14 μA/cm^2 ($P > 0.05$). Lastly, TFMP, a chloride channel inhibitor effective in inhibiting TMEM16A,[29] reduced Isc significantly by -0.3 ± 0.03 μA/cm^2 ($P < 0.05$). The relative percentage change relative to basal Isc caused by each drug was: amiloride, -20% $\pm 5.2\%$; phloridzin, $-39\% \pm 1.6\%$; forskolin, $+209\% \pm 19.4\%$; CFTRinh172, $-103\% \pm 9.2\%$; UTP, $+18\% \pm 4.9\%$; paxilline, $-15\% \pm 3.1\%$; and TFMP, $-10\% \pm 1.7\%$. This set of experiments demonstrated activity of multiple ion channels in primary rat MG cells.

FIGURE 8. Immunolocalization of the Na^+/K^+ ATPase in rat MG tissues, MG ALI cultures, and MG spheroid cultures. Positive Na^+/K^+ ATPase staining was localized to the plasma membrane of rat MG ductal epithelial and acinar cells. Similar plasma membrane immunoreactivity of Na^+/K^+ ATPase was observed in rat MG cells under ALI culture and spheroid culture.

## Functional Characterization of Rat MG Spheroid Cultures

We first tested volume responses of spheroid cultures to putative secretagogues 24 hours after drug addition. Vehicle addition did not cause detectable size changes (data not shown). In contrast, MG spheroids swelled in response to 10 μM forskolin treatment at 24 hours (Fig. 10A). Unexpectedly, MG spheroids shrank in response to 100 μM acetylcholine (Fig. 10B). We next tested for the Na^+/K^+ ATPase dependence of volume regulation (Fig. 11A). Ouabain produced a reduction in MG sphere volume, consistent with inhibition of basal volume secretion.

Second, we tested for a role for ENaC in mediating volume absorption. Inhibition of volume absorption by the ENaC inhibitor, benzamil, would be expected to produce swelling. In contrast, volume shrinkage was observed in response to benzamil (Fig. 11B).

To quantitate these responses, the baseline size of the spheroids was set at 100%, and the relative size of spheroids after 24 hours of drug treatment was calculated as percentage change from this baseline. This quantification revealed the following percentage volume changes: forskolin ($+140\%\ \pm$ 22.5%), acetylcholine ($-54\%\ \pm$ 7.5%), ouabain ($-67\%\ \pm$ 3.8%), and benzamil ($-63\%\ \pm$ 3.8%; Fig. 12). This study demonstrated roles for functional CFTR, ENaC, and the Na^+/K^+ ATPase in fluid fluxes in MG cells under 3D culture conditions.

DISCUSSION

Chloride secretion and sodium absorption provide the main driving forces for osmotically driven water movement across many epithelia throughout the body. Despite a large literature on the role of these chloride/sodium channels in the function of many mammalian glands, there is virtually no information on the role of ion channels in MG physiology. The first clue as to a
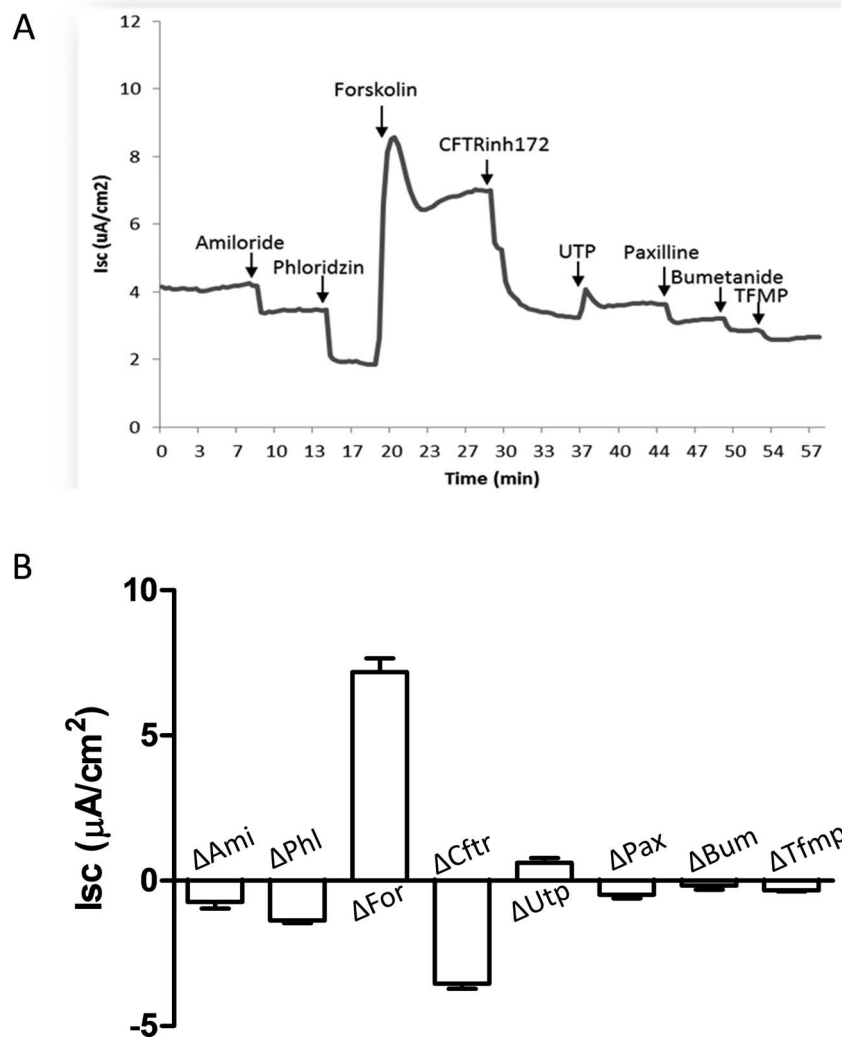
FIGURE 9. Ussing chamber studies of rat MG cell cultures to measure bioelectric properties. Drugs were applied in the following sequence: amiloride, phloridzin, forskolin, CFTRinh172, UTP, paxilline, bumetanide, and TFMP. All drugs were applied to the apical bath of chamber except bumetanide, which was applied to the serosal bath of chamber. (**A**) A representative Isc trace with the aforementioned serial drug treatments. (**B**) ΔIsc caused by each drug application ($n = 6$). Amiloride, phloridzin, CFTRinh172, paxillin, and TFMP inhibited Isc, whereas forskolin and UTP increased Isc significantly ($P < 0.05$). The Isc response to forskolin was the largest among all tested drugs.

potential role of these channels in MG function came from clinical research. Specifically, clinical reports indicate that PHA patients with genetic loss of ENaC function exhibit a MGD-like phenotype, with white material obstructing the MG orifice.[17–19] How absence of ENaC function produces this phenotype is not understood.

As an initial component of our investigation of MG ion transport, we studied the expression and localization of key ion transport proteins, e.g., βENaC, in the intact MG gland. We detected ENaC subunit mRNAs and protein in rat MG tissue (Figs. 1–3). In marked contrast with other epithelia in which *αENaC* is the dominant transcript, *βENaC* mRNA levels were significantly higher than *αENaC* and *γENaC* in rat MG. Again in contrast with other glands, in situ hybridization analysis revealed that all ENaC mRNAs were more abundantly expressed in acinar cells than ductular or ductal epithelial cells. The expression levels decreased from peripheral nonlumen facing acinar cells to the more mature acinar cells that line MG acinar structures (Fig. 2). Immunolocalization revealed a similar distribution of βENaC protein, with more intense signals in peripheral acinar cells. Considering MG's holocrine

secretion physiology, in which lumen facing acinar cells (meibocytes) rupture and secrete products into ductules, it is unclear whether ENaC (and other ion channels) exhibits functions related to transepithelial ion transport or cell maturation and tissue differentiation.[15,23,30]

The complex architecture of the MG tissue limits direct biophysical characterization of fresh MG tissues in Ussing chambers or volume responses as spheroids, which necessitated development of in vitro MG cell culture systems to perform functional studies. As a first step in the process, we used a recently reported protocol to "conditionally reprogram" the small number of cells obtained from freshly excised rat MG tissues.[20,21] Specifically, the combination of feeder cells and a ROCK inhibitor (Y-27632) enables cultured epithelial cells (e.g., prostate, mammary, and airway epithelial cells) to proliferate indefinitely, without the use of exogenous viral or cellular gene transduction.[20,31–33] The "conditionally reprogrammed cell (CRC)" phenotype is associated with an upregulated expression of adult stem cell genes including telomerase, α6/β1 intergrins, ΔNp63α, CD44, and telomerase reverse transcriptase.[20] Importantly, these CRCs can revert to
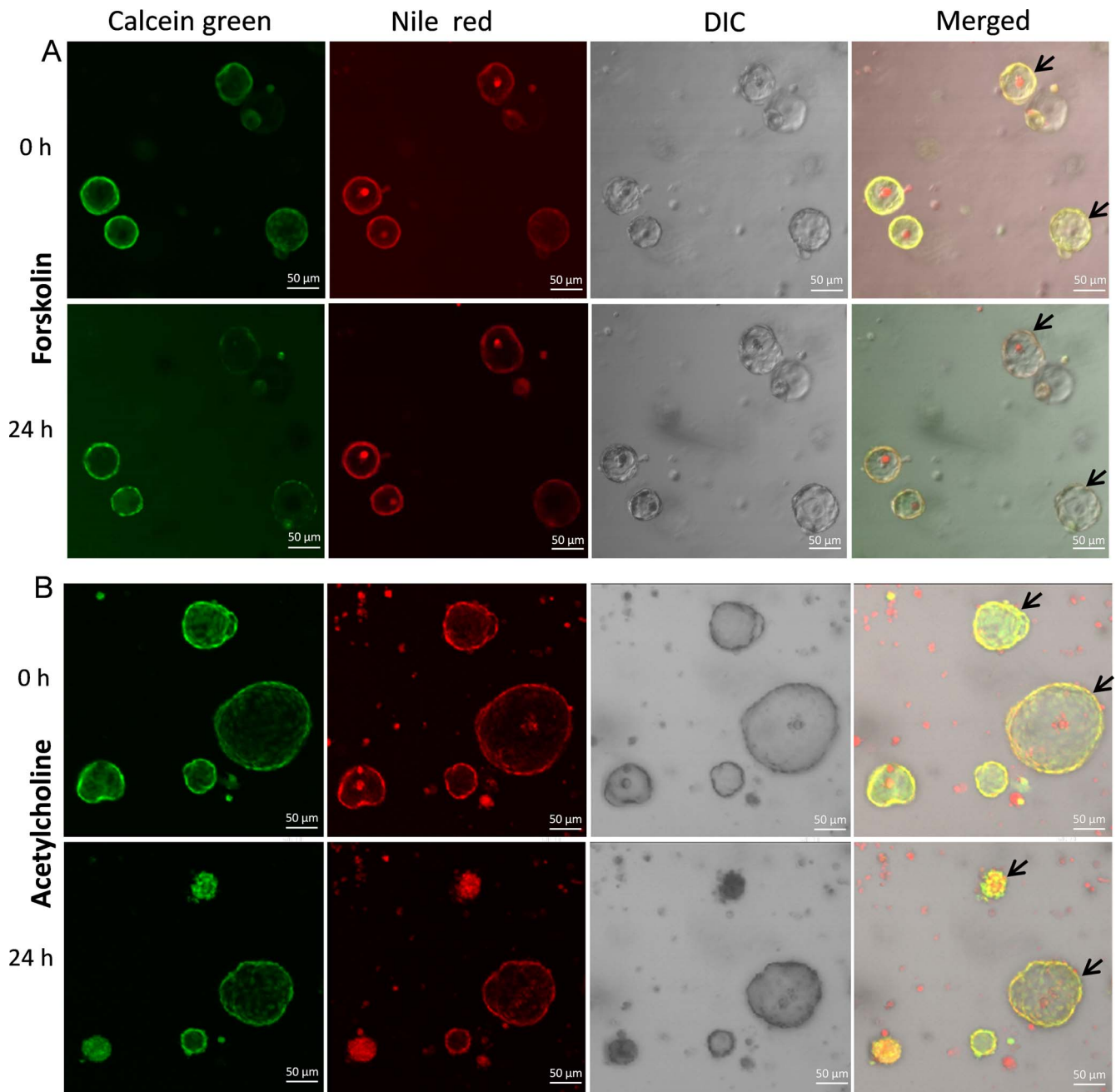
FIGURE 10. Effects of forskolin and acetylcholine on the volume of rat MG cell 3D cultures. **(A)** Representative confocal live-cell microscopy images of MG cell spheroids in response to 24 hours of 10 µM forskolin treatment. Calcein green labeled live cells and Nile Red labeled the lipid component of cell membrane or secretory products. *Arrows* indicate spheroids that swelled after 24 hours forskolin incubation. **(B)** Treatment with 100 µM acetylcholine for 24 hours caused rat MG cell spheroids shrinkage. DIC, differential interference contrast.

their original epithelial cell phenotype upon removal of feeder cells and Y-27632.

We induced cell differentiation of expanded MG cells under air-liquid interface planar culture conditions on permeable inserts by removal of feeder cells and Y-27632. Planar cultured MG cells accumulated neutral lipids in a pattern similar to rat MG tissues, suggesting preservation of basic MG acinar functions in culture (Fig. 6). The comparative mRNA analysis of planar cultures to freshly excised MG tissue for ion transport genes revealed similar levels of expression of some genes and disparity in others (Fig. 1B). We also examined the protein expression and localization of NKCC and Na^+/K^+ ATPase. The

distribution of both proteins was similar in cultured planar MG cells compared to freshly excised MG cells (Figs. 7, 8).

Importantly, there was evidence for vectorial transepithelial ion transport in MG ALI culture. Small amiloride-sensitive, ENaC-mediated Na^+ lumen to serosal absorption and a second Na^+ absorptive process, that is, phloridzin sensitive Na^+-glucose absorption, were detected. Note, *Slc5a1* mRNA was expressed much more abundantly in primary rat MG cell culture than freshly excised MG tissues (Fig. 1). Thus, although the magnitude of Na^+-glucose mediated Na^+ absorption exceeded that of ENaC mediated absorption in MG ALI culture, the relative roles of each Na^+ transport pathway in MG in vivo will require further study.
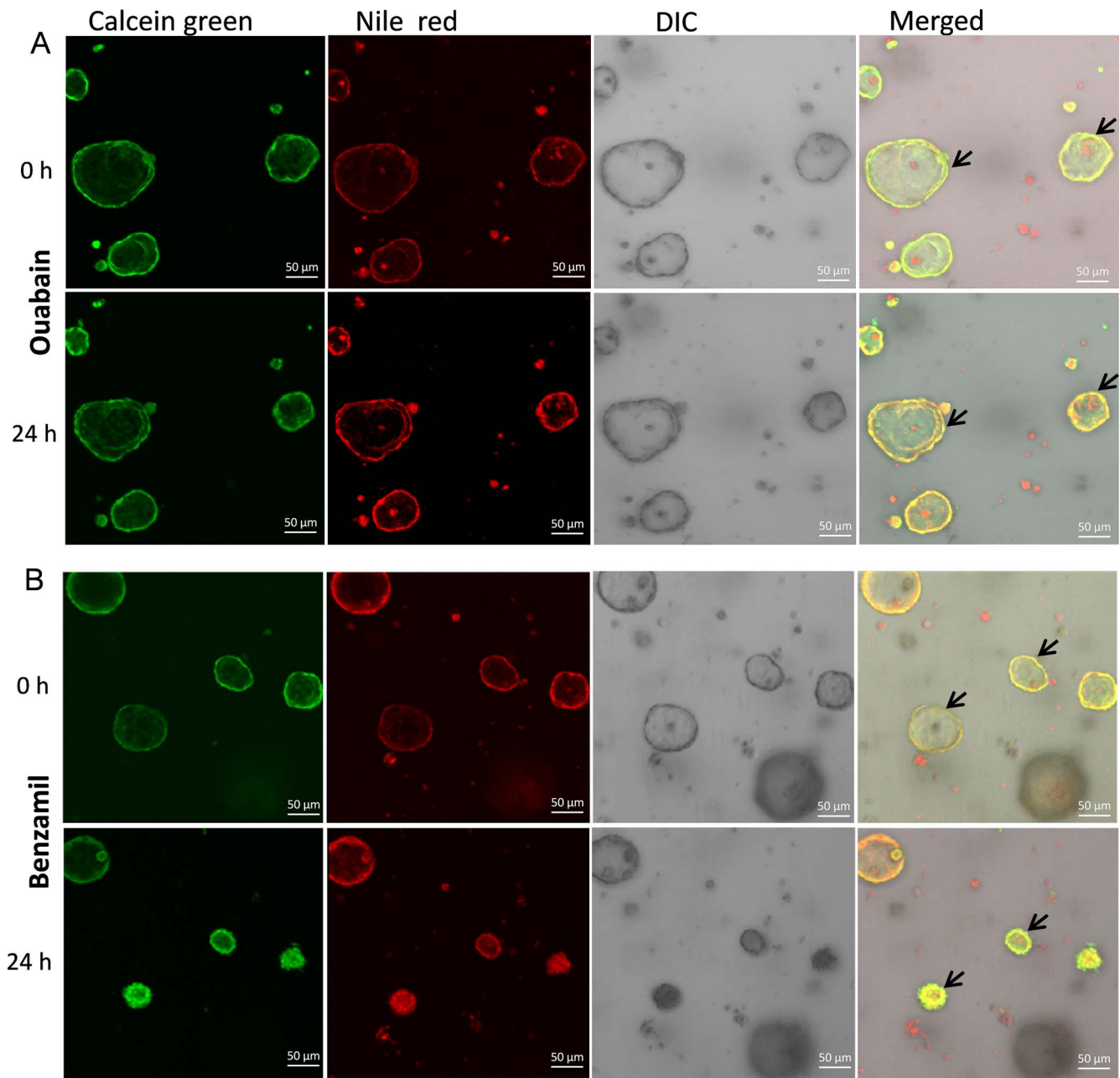
FIGURE 11. Effects of ouabain (**A**) and benzamil (**B**) on the volume of rat MG cell 3D spheroid cultures. Both 24 hours treatment of ouabain (**A**) and benzamil (**B**) induced rat MG cell spheroid shrinkage.

We also investigated Cl⁻ transport pathways in planar rat MG cultures. CFTR is a cAMP-activated chloride channel and potential regulator of other ion channels, including ENaC.[34] Functionally active CFTR has been identified in the cornea, conjunctiva, and lacrimal gland of the eye.[35-37] The importance of CFTR in ocular surface health has been proposed in several clinical studies of cystic fibrosis (CF) patients. For example, CF patients exhibit ocular abnormalities, including dry eye symptoms, compromised corneal epithelium integrity, decreased tear production and stability, and elevated tear inflammatory cytokines.[38-40] Cystic fibrosis transmembrane conductance regulator expression detected in intact MG gland was preserved in planar cultures (Fig. 1). Functional Ussing chamber studies of planar cultures detected robust Isc responses to the application of forskolin (CFTR activator)

and CFTRinh172 (CFTR inhibitor). These data suggested that MG cells in planar culture have a significant capacity of CFTR-mediated chloride and possible fluid secretion.

Chloride secretion in the acini of many glands is effected by Ca²⁺-mediated Cl⁻ channels, including TMEM16A. It has been well-documented that UTP and other nucleotide analogues have the capacity to accelerate the rate of conjunctival chloride/fluid secretion and conjunctival goblet cell mucin secretion.[41,42] TMEM16A has been identified as a Ca²⁺-activated chloride channels that may mediate UTP-activated Cl⁻ currents.[43,44] It also is possible that additional members of this family have similar functions, particularly TMEM16F.[45] Thus, we searched for and identified *Tmem16a* and *f* mRNA in rat MG tissues and planar cell cultures (Fig. 1). The rat MG cell cultures expressed statistically significant higher levels of
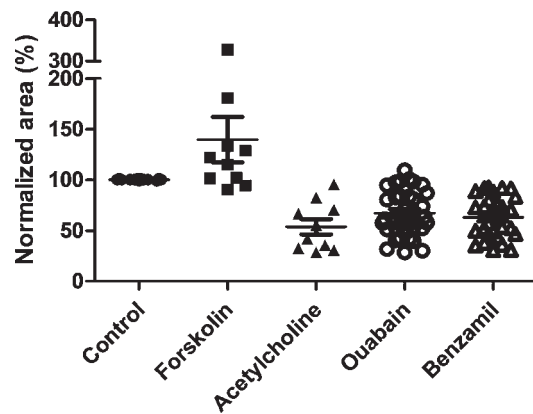
FIGURE 12. Mean area changes for MG spheroids after agonist and antagonist addition at 24 hours. Sizes of spheroids after forskolin, acetylcholine, ouabain, and benzamil addition were measured with Image J and normalized relative to that before drug treatment (100%, *n* = 10–36).

Tmem16a and *Tmem16f* mRNA than MG tissues. Pharmacologic studies with UTP/TFMP as activators/inhibitors of TMEM16A, however, provided evidence for only a very modest activity of Ca^{2+}-activated Cl$^-$ channel function in rat MG cell planar cultures.

To assess the relationship between transepithelial ion currents and volume flow, we developed 3D spheroid cultures in a matrigel matrix. The 3D culture system has the advantage of forming MG cell acinar-like spheroids that contain a cell population of acinar and possibly some ductal cells (Figs. 6, 7). Ultrastructural examination of MG 3D spheroids identified intracellular accumulation of lysosomal lamellar bodies (Fig. 5B), which are lysosomes specialized for lipid storage and secretion.[47] The abundance of lamellar bodies, together with nuclear pyknosis (Fig. 5B) and secretory products with cell debris inside the lumen, represents typical MG acinar cell terminal differentiation and holocrine secretion processes.[48,49] Consistent with an acinar activity in spheroids, the luminal contents of most spheroids contained Nile Red staining positive material (Fig. 6). However, the pattern of NKCC or Na$^+$/K$^+$ ATPase staining in spheroids (Fig. 7) could not rule out the presence of some ductal cells in the cell culture system.

We then performed studies to elucidate how the identified transepithelial ion transport processes might be integrated into MG gland physiology. Importantly, it is not clear that holocrine secretion into the acinar lumen requires transepithelial ion secretion as occurs in other glands, for example, the lacrimal gland. To compare the effect of potential CFTR-mediated volume transport with other gland spheroid preparations, for example, airway, intestine, forskolin induced effect on MG spheroid expansion were calculated. Spheroid expansion was observed with forskolin administration, consistent with CFTR-mediated Cl$^-$ and volume secretion (Figs. 10A, 12).[46] The effect of ouabain to induce the shrinkage of spheroids is consistent with a basolaterally located Na$^+$/K$^+$ ATPase that generates the appropriate trans-basolateral membrane ion gradients to drive Cl$^-$ into the cell for CFTR dependent trans-apical membrane Cl$^-$ secretion (Figs. 11A, 12). Future studies will be needed for a detailed description of the kinetics of forskolin-induced voluminal secretion in MG spheroids.

The MG has been reported previously to have abundant cholinergic innervation and might have been expected to exhibit cholinergically Ca^{2+} stimulated Cl$^-$ and volume secretion.[50,51] Our confocal study, however, suggested that cholinergic stimulation produced a decrease in volume. Such

an effect could reflect the dominance of Ca^{2+}-mediated K$^+$ absorption over Ca^{2+} mediated Cl$^-$ secretion.

We used an ENaC inhibitor, benzamil, as a probe to test the function of ENaC in MG function. The volume response to benzamil was perplexing. It would have been predicted that if Na$^+$ absorption from acinar lumens was a feature of MG acini, as evidenced by Ussing chamber data, that inhibition of this process would have induced spheroid expansion rather than reduction. The observation that benzamil reduced spheroid volume is consistent with: (1) inhibition of Na$^+$ transport from the peripheral acinar cells into the lumen, a response not consistent with the direction of Na$^+$ transport in Ussing chambers, or (2) a nonspecific inhibition of the basolateral Na$^+$/K$^+$ ATPase and secondary inhibition of Cl$^-$ and fluid secretion into the acinar lumen.[52]

Collectively, our data suggested that transepithelial Cl$^-$ and volume secretion may be an important and unrecognized component of MG acinar holocrine secretion. However, the peripheral acinar distribution of ENaC expression, coupled with the small component of amiloride sensitive Na$^+$ transport in planar cultures and absence of evidence for ENaC mediated volume absorption in spheroid cultures, make it unlikely that ENaC mediated absorption is important to re-absorb Na$^+$ released into the MG acinar/lumen during holocrine secretion. Rather, these observations, plus the uniquely high expression of βENaC in MG, raise the possibility that the loss of ENaC function in PHA subjects may produce the MG phenotype by a loss of an ENaC contribution to extracellular sensing/cell proliferation activities in MG acinar cells.

In summary, this study characterized the presence and function of selected ion channels in rat MG, including ENaC and CFTR. The unique distribution pattern of ENaC in MG suggested a role for ENaC in MG cell maturation and differentiation, as compared to the transepithelial Na$^+$ transport functions noted in corneal epithelial cells.[23] However, our studies of ALI cultures and spheroids argue for a role of CFTR mediated Cl$^-$ and fluid secretion in MG function. Use of transgenic mice to knock out specific ion channels will provide a better understanding of the specific roles of these ion channels in normal MG function and pathogenesis of MG dysfunction. Finally, our primary MG CRC culture approach provides a good platform to generate planar and spheroid model systems. As with other epithelial model systems, future studies may be required to adjust culture conditions to more precisely mimic gene expression patterns of freshly excised MG cells in CRC MG cells. Our data do suggest that the CRC approach may be useful for further translational studies that evaluate MG physiology and, perhaps, lead to a better understanding of MGD and development of MGD therapies.

S.H. Randell, Parion Sciences (F), Gilead Sciences (C); **R.C. Boucher**, Parion Sciences (I)

References

1. Knop E, Knop N, Millar T, Obata H, Sullivan DA. The international workshop on meibomian gland dysfunction: report of the subcommittee on anatomy, physiology, and pathophysiology of the meibomian gland. *Invest Ophthalmol Vis Sci*. 2011;52:1938–1978.

2. Schaumberg DA, Nichols JJ, Papas EB, Tong L, Uchino M, Nichols KK. The international workshop on meibomian gland dysfunction: report of the subcommittee on the epidemiology of, and associated risk factors for, MGD. *Invest Ophthalmol Vis Sci*. 2011;52:1994–2005.

3. Schaumberg DA, Dana R, Buring JE, Sullivan DA. Prevalence of dry eye disease among US men: estimates from the Physicians' Health Studies. *Arch Ophthalmol*. 2009;127:763–768.

4. Schaumberg DA, Sullivan DA, Buring JE, Dana MR. Prevalence of dry eye syndrome among US women. *Am J Ophthalmol*. 2003;136:318–326.

5. Ding J, Sullivan DA. Aging and dry eye disease. *Exp Gerontol*. 2012;47:483–490.

6. Moss SE, Klein R, Klein BE. Prevalence of and risk factors for dry eye syndrome. *Arch Ophthalmol*. 2000;118:1264–1268.

7. Han SB, Hyon JY, Woo SJ, Lee JJ, Kim TH, Kim KW. Prevalence of dry eye disease in an elderly Korean population. *Arch Ophthalmol*. 2011;129:633–638.

8. Hykin PG, Bron AJ. Age-related morphological changes in lid margin and meibomian gland anatomy. *Cornea*. 1992;11:334–342.

9. Nien CJ, Massei S, Lin G, et al. Effects of age and dysfunction on human meibomian glands. *Arch Ophthalmol*. 2011;129:462–469.

10. Nandoskar P, Wang Y, Wei R, et al. Changes of chloride channels in the lacrimal glands of a rabbit model of Sjogren syndrome. *Cornea*. 2012;31:273–279.

11. Ubels JL, Hoffman HM, Srikanth S, Resau JH, Webb CP. Gene expression in rat lacrimal gland duct cells collected using laser capture microdissection: evidence for K+ secretion by duct cells. *Invest Ophthalmol Vis Sci*. 2006;47:1876–1885.

12. Candia OA. Electrolyte and fluid transport across corneal, conjunctival and lens epithelia. *Exp Eye Res*. 2004;78:527–535.

13. Yu D, Thelin WR, Rogers TD, et al. Regional differences in rat conjunctival ion transport activities. *Am J Physiol Cell Physiol*. 2012;303:C767–C780.

14. Dartt DA. Regulation of mucin and fluid secretion by conjunctival epithelial cells. *Prog Retin Eye Res*. 2002;21:555–576.

15. Grifoni SC, Gannon KP, Stec DE, Drummond HA. ENaC proteins contribute to VSMC migration. *Am J Physiol Heart Circ Physiol*. 2006;291:H3076–H3086.

16. Justet C, Evans F, Vasilskis E, Hernandez JA, Chifflet S. ENaC contribution to epithelial wound healing is independent of the healing mode and of any increased expression in the channel. *Cell Tissue Res*. 2013;353:53–64.

17. Ainsworth JR, Ramsay AS, Galea P, Diaper C. Disordered meibomian gland function in pseudohypoaldosteronism. *Arch Ophthalmol*. 1996;114:1018–1019.

18. Eliwa MS, El-Emmawie AH, Saeed MA. Ocular and skin manifestations in systemic pseudohypoaldosteronism. *BMJ Case Rep*. 2014;2014.

19. Nasir A, Najab IA. Unique eyelid manifestations in type 1 pseudohypoaldosteronism. *Arch Dis Child Fetal Neonatal Ed*. 2012;97:F462.

20. Suprynowicz FA, Upadhyay G, Krawczyk E, et al. Conditionally reprogrammed cells represent a stem-like state of adult epithelial cells. *Proc Natl Acad Sci U S A*. 2012;109:20035–20040.

21. Liu S, Hatton MP, Khandelwal P, Sullivan DA. Culture, immortalization, and characterization of human meibomian gland epithelial cells. *Invest Ophthalmol Vis Sci*. 2010;51:3993–4005.

22. Matsushima D, Heavner W, Pevny LH. Combinatorial regulation of optic cup progenitor cell fate by SOX2 and PAX6. *Development*. 2011;138:443–454.

23. Tucker ES, Segall S, Gopalakrishna D, et al. Molecular specification and patterning of progenitor cells in the lateral and medial ganglionic eminences. *J Neurosci*. 2008;28:9504–9518.

24. Maskin SL, Tseng SC. Culture of rabbit meibomian gland using collagen gel. *Invest Ophthalmol Vis Sci*. 1991;32:214–223.

25. Kutsuna M, Kodama T, Sumida M, et al. Presence of adipose differentiation-related protein in rat meibomian gland cells. *Exp Eye Res*. 2007;84:687–693.

26. Bancroft JD, Stevens A. *Theory and Practice of Histological Techniques*. 3rd ed. New York: Churchill Livingstone; 1990.

27. Lotowska JM, Sobaniec-Lotowska ME, Bockowska SB, Lebensztejn DM. Pediatric non-alcoholic steatohepatitis: the first report on the ultrastructure of hepatocyte mitochondria. *World J Gastroenterol*. 2014;20:4335–4340.

28. Burch LH, Talbot CR, Knowles MR, Canessa CM, Rossier BC, Boucher RC. Relative expression of the human epithelial Na+ channel subunits in normal and cystic fibrosis airways. *Am J Physiol*. 1995;269:C511–C518.

29. Oh SJ, Park JH, Han S, Lee JK, Roh EJ, Lee CJ. Development of selective blockers for Ca(2)(+)-activated Cl channel using Xenopus laevis oocytes with an improved drug screening strategy. *Mol Brain*. 2008;1:14.

30. Xu W, Hong SJ, Zeitchek M, et al. Hydration status regulates sodium flux and inflammatory pathways through epithelial sodium channel (ENaC) in the skin. *J Invest Dermatol*. 2015;135:796–806.

31. Chapman S, Liu X, Meyers C, Schlegel R, McBride AA. Human keratinocytes are efficiently immortalized by a Rho kinase inhibitor. *J Clin Invest*. 2010;120:2619–2626.

32. Liu X, Ory V, Chapman S, et al. ROCK inhibitor and feeder cells induce the conditional reprogramming of epithelial cells. *Am J Pathol*. 2012;180:599–607.

33. Bove PF, Dang H, Cheluvaraju C, et al. Breaking the in vitro alveolar type II cell proliferation barrier while retaining ion transport properties. *Am J Respir Cell Mol Biol*. 2014;50:767–776.

34. Gentzsch M, Dang H, Dang Y, et al. The cystic fibrosis transmembrane conductance regulator impedes proteolytic stimulation of the epithelial Na+ channel. *J Biol Chem*. 2010;285:32227–32232.

35. Sun XC, Bonanno JA. Expression, localization, and functional evaluation of CFTR in bovine corneal endothelial cells. *Am J Physiol Cell Physiol*. 2002;282:C673–C683.

36. Turner HC, Bernstein A, Candia OA. Presence of CFTR in the conjunctival epithelium. *Curr Eye Res*. 2002;24:182–187.

37. Ding C, Parsa L, Nandoskar P, Zhao P, Wu K, Wang Y. Duct system of the rabbit lacrimal gland: structural characteristics and role in lacrimal secretion. *Invest Ophthalmol Vis Sci*. 2010;51:2960–2967.

38. Sheppard JD, Orenstein DM, Chao CC, Butala S, Kowalski RP. The ocular surface in cystic fibrosis. *Ophthalmology*. 1989;96:1624–1630.

39. Kalayci D, Kiper N, Ozcelik U, Gocmen A, Hasiripi H. Clinical status, ocular surface changes and tear ferning in patients with cystic fibrosis. *Acta Ophthalmol Scand*. 1996;74:563–565.

40. Mrugacz M, Kaczmarski M, Bakunowicz-Lazarczyk A, Zelazow-ska B, Wysocka J, Minarowska A. IL-8 and IFN-gamma in tear fluid of patients with cystic fibrosis. *J Interferon Cytokine Res*. 2006;26:71–75.

41. Jumblatt JE, Jumblatt MM. Regulation of ocular mucin secretion by P2Y2 nucleotide receptors in rabbit and human conjunctiva. *Exp Eye Res*. 1998;67:341–346.

42. Li Y, Kuang K, Yerxa B, Wen Q, Rosskothen H, Fischbarg J. Rabbit conjunctival epithelium transports fluid, and P2Y2(2) receptor agonists stimulate Cl(-) and fluid secretion. *Am J Physiol Cell Physiol*. 2001;281:C595–C602.

43. Almaca J, Tian Y, Aldehni F, et al. TMEM16 proteins produce volume-regulated chloride currents that are reduced in mice lacking TMEM16A. *J Biol Chem*. 2009;284:28571–28578.

44. Caputo A, Caci E, Ferrera L, et al. TMEM16A, a membrane protein associated with calcium-dependent chloride channel activity. *Science*. 2008;322:590–594.

45. Pedemonte N, Galietta LJ. Structure and function of TMEM16 proteins (anoctamins). *Physiol Rev*. 2014;94:419–459.

46. Dekkers JF, Wiegerinck CL, de Jonge HR, et al. A functional CFTR assay using primary cystic fibrosis intestinal organoids. *Nat Med*. 2013;19:939–945.

47. Takahashi K, Naito M. Lipid storage disease: Part II. Ultrastructural pathology of lipid storage cells in sphingolip-idoses. *Acta Pathol Jpn*. 1985;35:385–408.

48. Knop N, Knop E. Meibomian glands. Part I: anatomy, embryology and histology of the Meibomian glands [in German]. *Ophthalmologe*. 2009;106:872–883.

49. Jester JV, Rajagopalan S, Rodrigues M. Meibomian gland changes in the rhino (hrrhhrrh) mouse. *Invest Ophthalmol Vis Sci*. 1988;29:1190–1194.

50. Zhu HY, Riau AK, Barathi VA, Chew J, Beuerman RW. Expression of neural receptors in mouse meibomian gland. *Cornea*. 2010;29:794–801.

51. LeDoux MS, Zhou Q, Murphy RB, Greene ML, Ryan P. Parasympathetic innervation of the meibomian glands in rats. *Invest Ophthalmol Vis Sci*. 2001;42:2434–2441.

52. Soltoff SP, Mandel LJ. Amiloride directly inhibits the Na,K-ATPase activity of rabbit kidney proximal tubules. *Science*. 1983;220:957–958.